

Weakly bound carbon-hydrogen complex in silicon

L. Hoffmann, E. V. Lavrov,* and B. Bech Nielsen

Institute of Physics and Astronomy, Aarhus University, DK-8000 Aarhus C, Denmark

B. Hourahine and R. Jones

Department of Physics, University of Exeter, Exeter EX4 4QL, United Kingdom

S. Öberg

Department of Mathematics, Luleå University of Technology, S-95187 Luleå, Sweden

P. R. Briddon

Department of Physics, The University of Newcastle upon Tyne, Newcastle upon Tyne NE1 7RU, United Kingdom

(Received 1 February 2000)

Local vibrational modes of a weakly bound carbon-hydrogen complex in silicon have been identified with infrared-absorption spectroscopy. After implantation of protons at ~ 20 K and subsequent annealing at 180 K, two carbon modes at 596 and 661 cm^{-1} , and one hydrogen mode at 1885 cm^{-1} are observed. The three modes originate from the same complex, which is identified as bond-centered hydrogen in the vicinity of a nearby substitutional carbon atom. *Ab initio* theory has been applied to calculate the structure and local modes of carbon-hydrogen complexes with hydrogen located at the first, second, and third nearest bond-center site to substitutional carbon. The results support our assignment.

I. INTRODUCTION

Carbon and hydrogen impurities take part in a number of point defects in crystalline silicon, among which the most prominent are substitutional carbon,¹ C_s , and bond-centered hydrogen,^{2,3} H_{BC} both of which have been characterized previously. Recently, also carbon-hydrogen complexes in silicon have been addressed.⁴⁻¹³ The formation of such complexes may significantly reduce the migration of hydrogen and, thus, be of technological importance. So far only a few carbon-hydrogen complexes have been observed by deep-level transient spectroscopy (DLTS),⁴⁻⁶ photoluminescence,^{7,8} and infrared-absorption spectroscopy.^{9,10}

In the present study, carbon-hydrogen complexes of low thermal stability have been studied by infrared-absorption spectroscopy. Previously, an electrically active carbon-hydrogen complex of low thermal stability was observed in *n*-type silicon by DLTS.^{4,5} The complex, *E3*, was assigned to a hydrogen atom bound to a C_s and located between the carbon atom and one of its four silicon neighbors [denoted $(C_s H_{BC})Si$].⁵ In *p*-type silicon a thermally more stable complex, named *H1*, was observed,⁶ which was assigned to a hydrogen atom occupying one of the antibonding sites of C_s [denoted $(H_{AB}C_s)Si$]. These complexes have been investigated by *ab initio* calculations,¹¹⁻¹³ and it was found that $(C_s H_{BC})Si$ is the most stable structure for the neutral and positive charge states, whereas $(H_{AB}C_s)Si$ is energetically favored for the negative charge state. In this work, carbon-hydrogen complexes are produced by low-temperature proton implantation into carbon-rich silicon. Infrared-absorption spectroscopy is applied to investigate the local vibrational modes of these complexes. Three correlated hydrogen- and carbon-related modes are observed. From the experimental findings and *ab initio* calculations, we identify the complexes

as a H_{BC}^+ in the vicinity of a nearby C_s atom but not directly bound to C_s . The infrared lines are then assigned to a defect that has not been considered previously.

II. EXPERIMENTAL

Samples with typical dimensions of $8 \times 8 \times 1.7$ mm² were cut from high-resistivity float-zone silicon crystals, which were either undoped (Fz-Si) or doped with ¹²C (Si:¹²C). In addition, a few samples were cut from a silicon crystal doped with ¹³C (Si:¹³C). This crystal was *n*-type with a resistivity of 10 Ω cm, corresponding to a phosphorus concentration of 4×10^{14} cm⁻³. The concentration of carbon and oxygen atoms were estimated from the intensities, measured at 9 K, of the local modes of ¹² C_s at 607 cm^{-1} (or ¹³ C_s at 589 cm^{-1}) and of interstitial oxygen (¹⁶O_i) at 1136 cm^{-1} (see Ref. 14). The Fz-Si samples contained less than 5×10^{15} cm⁻³ oxygen and carbon atoms. The Si:¹²C samples contained 4.5×10^{17} cm⁻³ of ¹²C and 1×10^{16} cm⁻³ of ¹⁶O atoms. The Si:¹³C samples contained 8.0×10^{17} cm⁻³ of ¹³C, 1×10^{17} cm⁻³ of ¹²C and 1×10^{17} cm⁻³ of ¹⁶O atoms.

The samples were mounted directly on the cold finger of a closed-cycle helium-cryocooler, which was capable of cooling the samples to 9 K. The samples were doped with hydrogen (Si:C:H) or deuterium (Si:C:D) by implantation of protons or deuterons through a 100- μ m-thick aluminum window in the vacuum shield of the cryostat. Both opposing 8×8 mm² faces of the samples were implanted at many different energies: 64 in the case of protons and 46 in the case of deuterons. The dose implanted at each energy was adjusted to yield an almost uniform depth distribution of implants. The local concentration of hydrogen or deuterium was 6×10^{16} cm⁻³, and the depth profile extended from the surfaces of the sample to a depth of 740 μ m for protons and

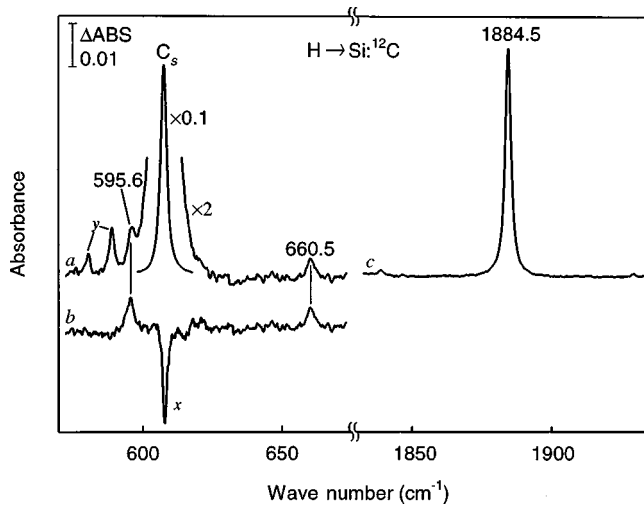


FIG. 1. Sections of absorbance spectra measured on a Si: ^{12}C :H sample annealed at 180 K. The spectra are shown after subtraction of spectra recorded on (curve *a*) Fz-Si, (curve *b*) Si: ^{12}C :H annealed at 240 K, and (curve *c*) background containing water. The line denoted *x* in curve *b* originates from a slightly different concentration of C_s at 180 and 240 K. The lines denoted *y* are carbon related (unidentified), but display a different annealing behavior than the lines studied in this work and thus, do not originate from the present complex. The weak line at 1838 cm^{-1} originates from H_2^* (Ref. 28).

$420\text{ }\mu\text{m}$ for deuterons. One sample (Si:C:H+D) was co-implanted with both isotopes in overlapping profiles extending from the surfaces to a depth of $420\text{ }\mu\text{m}$. In this case the local concentration of each isotope was $6 \times 10^{16}\text{ cm}^{-3}$. This hydrogen concentration was chosen because it yielded the maximum intensities of the local vibrational modes of interest to this work. During implantation the beam was swept horizontally and vertically across the sample to ensure a homogeneous lateral distribution of implants. At each energy the beam flux was determined before the implantation from the current measured in a calibrated beam cup located just in front of the sample, and the implantation time was then calculated to yield the desired dose. The maximum temperature was 20 K and the background pressure was 5×10^{-6} Torr during implantation.

After the implantation, the helium cryostat was moved to the infrared spectrometer. The turbopump and the cryocooler were switched off during the transport. However, for none of the samples did the temperature rise above 20 K before the cryocooler was restarted. Then the vacuum shield was rotated by 90° , without breaking the vacuum, and the infrared transmission spectrum was measured through two 4-mm-thick CsI windows in the shield.

A heater mounted on the same copper block as the sample was used to perform a series of heat treatments (annealings). During each treatment the temperature was stable to within $\pm 2^\circ\text{C}$, and the annealing time was 30 min. The first annealing was carried out at 40 K, and in each subsequent annealing step the temperature was increased by 20 K. After each step the infrared-absorption spectrum was recorded at 9 K.

The infrared-absorption measurements were performed with a Nicolet System 800 Fourier-transform spectrometer, which in the present configuration covers the spectral range

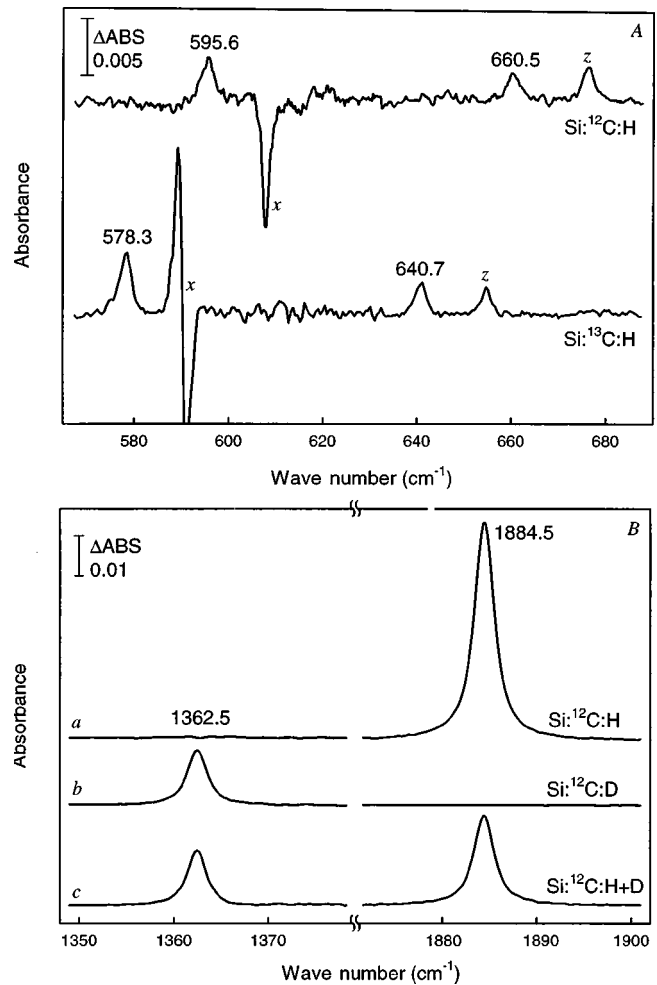


FIG. 2. Sections of absorbance spectra measured on A) Si: ^{12}C :H and Si: ^{13}C :H after annealing at 180 K, and B) Si: ^{12}C :H, Si: ^{12}C :D and Si: ^{12}C :H+D after annealing at 180 K for the 1884.5-cm^{-1} line and 200 K for the 1362.5-cm^{-1} line. The lines denoted *x* originate from a slightly different concentration of C_s in the spectrum and the in the reference spectrum. The lines denoted *z* are carbon related (unidentified), but display a different annealing behavior than the lines studied in this work and thus, do not originate from the present complex.

from 450 to 7000 cm^{-1} . A Ge-KBr beamsplitter, a global light source, and a MCT (mercury-cadmium-telluride) detector was applied. The apodized resolution was 1 cm^{-1} , and the sample temperature was 9 K during measurements.

All spectra have been subtracted by a reference spectrum. In the spectral range $450\text{--}1000\text{ cm}^{-1}$, the reference absorbance spectra were recorded on the implanted samples after annealing at 240 K. The absorption lines investigated in this work disappear after annealing at 240 K. In the spectral range $1000\text{--}2000\text{ cm}^{-1}$, the reference spectrum contained intense water lines and was measured without any sample.

III. RESULTS

In Fig. 1 sections of absorbance spectra measured after low-temperature proton implantation of Si: ^{12}C and subsequent annealing at 180 K are shown. Three new lines, which are absent in Fz-Si, are seen. Two of the lines are rather weak and are located at 596 and 661 cm^{-1} , close to the 607

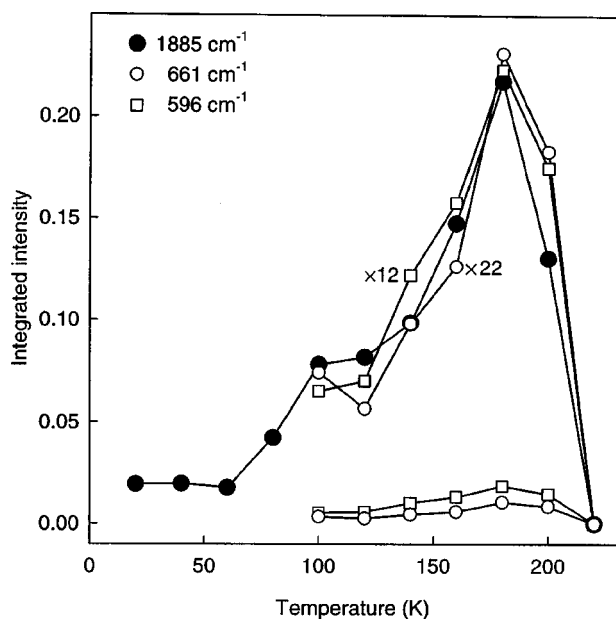


FIG. 3. Intensities of the 596-, 661-, and 1885- cm^{-1} modes shown against annealing temperature. The intensities of the 596- and 661- cm^{-1} modes have been scaled by a factor of 12 and 22, respectively. The 596- and 661- cm^{-1} modes cannot be resolved at annealing temperatures below 100 K.

cm^{-1} mode of C_s .¹ However, after subtraction of a reference spectrum, which contains the C_s line, the two lines are clearly resolved (see curve *b*). The third line is much more intense and is located at 1885 cm^{-1} , fairly close to the 1998- cm^{-1} mode of H_{BC}^+ .¹⁵

When ^{12}C is substituted by ^{13}C , the 596- and 661- cm^{-1} lines shift down in frequency to 578 and 641 cm^{-1} , as can be seen from Fig. 2(A). The frequency ratio between the corresponding lines in ^{12}C - and ^{13}C -doped material is on average 1.030. For a carbon atom bound to a silicon atom by a harmonic spring, the expected ratio is $\sqrt{m_r^{13}/m_r^{12}} = 1.028$, where m_r^α ($\alpha = 12, 13$) is the reduced mass of a $\text{Si}-\alpha\text{C}$ molecule. The close agreement between the two ratios strongly suggests that the 596- and 661- cm^{-1} lines represent local vibrational modes of carbon bound to one or more silicon atoms.

The 1885- cm^{-1} line shifts to 1363 cm^{-1} when deuterons are implanted instead of protons [see Fig. 2(B)]. The frequency ratio between these two lines is 1.38, which is close to the ratio 1.39 expected for a hydrogen atom attached to a silicon atom by a harmonic spring. This demonstrates that the 1885- cm^{-1} line represents a local vibrational mode of hydrogen bound to a heavier element, which most likely is silicon. One of the ^{12}C -doped samples was co-implanted with protons and deuterons in overlapping profiles to obtain information on the number of hydrogen atoms involved in the complex. Apart from the modes observed in a sample implanted with a single hydrogen isotope, no additional modes were observed (see Fig. 2(B), curve *c*). Hence, the 1885- cm^{-1} mode originates from a center, which involves a single hydrogen atom.

The annealing behavior of the hydrogen and the two carbon local modes are shown in Fig. 3. The hydrogen mode at 1885 cm^{-1} is observed as a rather weak line immediately after the implantation. However, as the temperature is raised

TABLE I. Local mode frequencies (cm^{-1}) of the CH_1 complex.

Mode	Sample			
	$^{12}\text{C}:\text{H}$	$^{12}\text{C}:\text{D}$	$^{13}\text{C}:\text{H}$	$^{13}\text{C}:\text{D}$
H	1884.5	1362.5	1884.3	1362.3
C	660.5	660.0	640.7	639.9
C	595.6	595.3	578.3	577.8

its intensity increases significantly. The mode attains maximum intensity after annealing at 180 K and disappears after annealing at 220 K. The weak carbon modes at 596 and 661 cm^{-1} cannot be resolved at annealing temperatures below 100 K. These modes also reach maximum intensity after annealing at 180 K and disappear at 220 K. As can be seen from the figure, the annealing behavior of the 596-, 661-, and 1885- cm^{-1} modes are identical for annealing temperatures in the range from 100 to 220 K. Therefore, we conclude that the three modes originate from the same carbon-hydrogen complex, which we denote CH_1 . No other absorption lines in our spectra display similar annealing dependence.

Isotope substitution may also be used to obtain information on the coupling between the carbon and hydrogen atoms. In Table I the frequencies of the carbon and hydrogen modes are compiled for the different combinations of carbon and hydrogen isotopes investigated in this work. The hydrogen and deuterium modes shift only by -0.2 cm^{-1} when ^{12}C is substituted by ^{13}C . Although such a small shift is at the limit of what our spectra allows us to resolve, we believe this shift is real. The local mode of H_{BC}^+ at 1998 cm^{-1} does not shift when ^{12}C is replaced by ^{13}C . The carbon modes at 596 (or 578) and 661 (or 641) cm^{-1} shift down in frequency by $\sim 0.5 \text{ cm}^{-1}$ when hydrogen is substituted by deuterium in a sample doped with ^{12}C (or ^{13}C) (see Fig. 4). These shifts are real and are not caused by, e.g., the reference subtraction. We note that the carbon-related mode at 676.4 cm^{-1} (or 654.7 cm^{-1} in Si^{13}C), denoted *z* in Fig. 2(A), does not shift. On this basis, we conclude that the hydrogen and carbon atoms in CH_1 are weakly dynamically coupled.

There is evidence for a second carbon-hydrogen complex

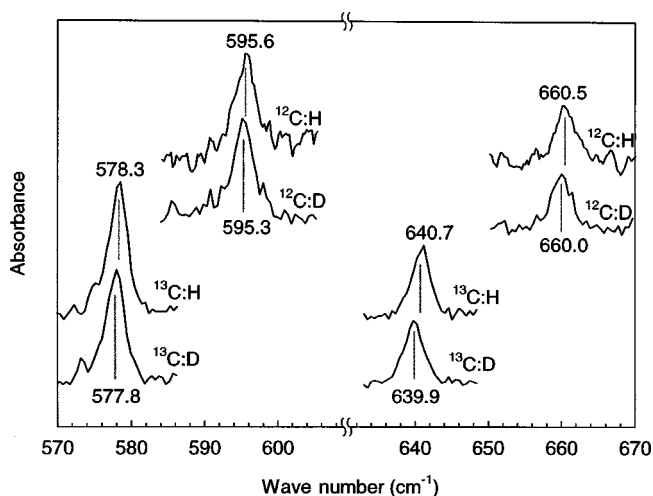


FIG. 4. Sections of absorbance spectra recorded on $\text{Si}^{12}\text{C}:\text{H}$, $\text{Si}^{12}\text{C}:\text{D}$, $\text{Si}^{13}\text{C}:\text{H}$, and $\text{Si}^{13}\text{C}:\text{D}$. The straight lines show the frequencies of the local vibrational modes.

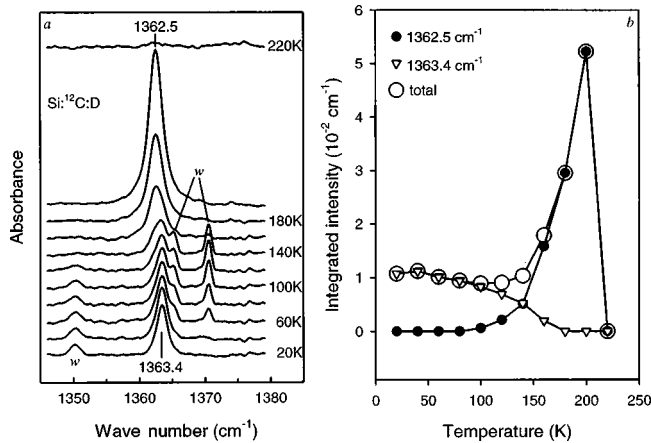


FIG. 5. (a) Annealing behavior of the 1362.5- and 1363.4- cm^{-1} modes. The lines denoted w are observed in deuterium implanted Fz-Si and do not originate from the complexes studied in this work. (b) The intensities of the 1362.5- and 1363.4- cm^{-1} modes and the sum of the intensities of the two modes are shown against annealing temperature.

in our spectra. As mentioned above, the 1884.5- cm^{-1} hydrogen mode is seen as a weak line immediately after the implantation, whereas the 1362.5- cm^{-1} deuterium mode is observed only after annealing at temperatures above 100 K. However, a weak deuterium mode at 1363.4 cm^{-1} is observed just after the implantation. This mode has maximum intensity just after the implantation and anneals at ~ 160 K as can be seen from Fig. 5. The hydrogen counterpart of the 1363.4- cm^{-1} mode may be located on top of the 1884.5- cm^{-1} mode, which would explain why this mode is observed just after the implantation. Actually, in the Si- $^{12}\text{C}:\text{H}$ samples the mode is observed at 1884.6 cm^{-1} just after the implantation and shifts slightly to 1884.5 cm^{-1} after annealing at about 80 K. Due to the very small frequency shift, it has been impossible to disentangle the annealing dependencies of the 1884.5- and 1885.6- cm^{-1} modes. No carbon modes with the same annealing behavior as the 1363.4- cm^{-1} mode has been resolved. Because the intensity of this mode is very low, we expect that any correlated carbon mode will be impossible to detect with our setup. The fact that the 1363.4- cm^{-1} mode is observed only in carbon-rich material suggests that this mode is carbon related. Therefore, we shall henceforth refer to the associated center by the label CH_{II} . Finally, we note that the frequency of the 1363.4- cm^{-1} mode does not shift when ^{12}C is substituted by ^{13}C . Hence, the dynamical coupling between the hydrogen and carbon atoms in CH_{II} is very small.

IV. THEORETICAL CALCULATIONS

Recently, two oxygen-hydrogen complexes, formed after low-temperature proton implantation in Czochralski-grown silicon, have been reported.¹⁵ The two defects are thermally rather unstable and anneal at 130 and 240 K. They were identified as H_{BC}^+ trapped by the strain field of an interstitial oxygen atom, O_i . The properties of these defects resemble those of CH_I and CH_{II} presented above, indicating that H_{BC}^+ may become trapped also in the neighborhood of C_s . To substantiate this idea, we have therefore calculated the struc-

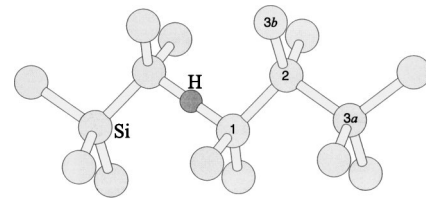


FIG. 6. Sketch of the $(\text{C}_s\text{H}_{\text{BC}}^+)_n$ ($n = 1, 2, 3a, 3b$) configurations. To obtain the configuration $(\text{C}_s\text{H}_{\text{BC}}^+)_n$, the silicon atom labeled n has been substituted by a carbon atom.

ture and the local mode frequencies of such $\text{C}_s\text{H}_{\text{BC}}^+$ complexes using an *ab initio* cluster technique.

A. Method

The method is based on local-density-functional pseudo-potential theory, and uses a basis of Gaussian orbitals.^{16,17} A 134-atom trigonal bond-centered cluster with composition $\text{Si}_{68}\text{H}_{66}$ was used. The wave functions were expanded in N atom-sited s and p Gaussian orbitals, while the charge density was expanded in M atom-sited s Gaussian functions. The (N, M) values used at each atomic site were (8, 8) for silicon and carbon sites, (2, 3) on the sites of surface hydrogen, and (3, 4) on the sites of the inner hydrogen atom. The Gaussian orbitals were treated as independent for all atoms except the hydrogen terminators, where a fixed linear combination was applied. In addition, three s and p Gaussian orbitals with different exponents were placed at each bond center—including those between the inner hydrogen atom and its silicon neighbors in the cluster. During energy minimization all atoms were allowed to relax. First, a cluster with an inner H_{BC}^+ was relaxed. Subsequently, a C_s was added to the relaxed cluster at various distances from the H_{BC}^+ . The four different configurations indicated in Fig. 6 were investigated: $(\text{C}_s\text{H}_{\text{BC}}^+)_1$, $(\text{C}_s\text{H}_{\text{BC}}^+)_2$, $(\text{C}_s\text{H}_{\text{BC}}^+)_3a$, and $(\text{C}_s\text{H}_{\text{BC}}^+)_3b$. $(\text{C}_s\text{H}_{\text{BC}}^+)_1$ is a trigonal defect (C_{3v}) with C_s neighboring H_{BC}^+ and $(\text{C}_s\text{H}_{\text{BC}}^+)_2$ has monoclinic-I symmetry (C_{1h}) with C_s located as nearest neighbor to one of the silicon atoms adjacent to H_{BC}^+ . $(\text{C}_s\text{H}_{\text{BC}}^+)_3a$ and $(\text{C}_s\text{H}_{\text{BC}}^+)_3b$ have monoclinic-I (C_{1h}) and triclinic (C_1) symmetry, respectively. For these two configurations, C_s is located as second nearest neighbor to one of the two silicon atoms adjacent to H_{BC}^+ .

B. Results

A single proton, placed at a bond center near to the middle of the cluster (without a carbon atom) resulted in Si-H bonds of length 1.647 and 1.635 Å and a Si-H-Si angle of 178°. The deviation from D_{3d} symmetry reflects the influence of surface on the defect. The hydrogen-related local vibrational mode lay at 1852 cm^{-1} , somewhat below that observed at 1998 cm^{-1} . The 7% underestimate in the frequency is typical of the method.

A single carbon atom placed in the silicon cluster at a site adjacent to the center of the cluster (without an inner hydrogen atom) resulted in C-Si bond lengths of 2.020, 2.020, 2.020, and 2.025 Å. The local vibrational modes were 581, 580, and 574 cm^{-1} . The 7- cm^{-1} splitting was due to the

TABLE II. Local vibrational modes in cm^{-1} of $(\text{C}_s\text{H}_{\text{BC}}^+)_n$ for $n=1,2,3a,3b$ obtained from the cluster calculation.

	Point group	$^{12}\text{C}:\text{H}$	$^{12}\text{C}:\text{D}$	$^{13}\text{C}:\text{H}$	$^{13}\text{C}:\text{D}$
H_{BC}^+	C_{3v}	1852.1	1316.2		
C_s		~ 578			
$(\text{C}_s\text{H}_{\text{BC}}^+)_1$	C_{3v}				
H mode		2624.1	1928.1	2616.3	1916.8
		1424.7	1049.0	1421.0	1042.8
		1413.3	1042.0	1409.4	1035.4
C mode		566.1	555.3	554.1	546.2
		556.6	548.9	548.9	543.2
		555.2	545.9	544.0	537.7
$(\text{C}_s\text{H}_{\text{BC}}^+)_2$	C_{1h}				
H mode		1795.0	1275.3	1794.9	1275.3
C mode		642.6	642.5	623.7	623.5
		574.1	571.6	561.8	559.1
		558.6	555.4	546.5	542.8
$(\text{C}_s\text{H}_{\text{BC}}^+)_3a$	C_{1h}				
H mode		1706.8	1214.7	1706.8	1214.7
		952.5	712.4	952.5	712.0
C mode		661.2	660.3	641.6	641.0
		609.5	609.3	592.7	592.6
		597.7	597.6	581.3	581.3
$(\text{C}_s\text{H}_{\text{BC}}^+)_3b$	C_1				
H mode		1802.3	1282.0	1802.3	1282.0
		823.2	653.2	823.2	634.8
C mode		652.9	625.8	633.8	625.0
		605.0	605.0	588.7	588.7
		597.3	597.2	581.0	580.9

distortion from T_d symmetry caused by the cluster geometry. These results are close to the observed three-dimensional T_2 mode at 607 cm^{-1} (Ref. 1).

We then consider complexes with carbon and hydrogen, finding $(\text{C}_s\text{H}_{\text{BC}}^+)_1$ to possess the lowest energy. This is $\sim 0.2 \text{ eV}$ lower than the energy of $(\text{C}_s\text{H}_{\text{BC}}^+)_n$ for $n=2,3a,3b$. If the zero-point energy is taken into account this energy difference is reduced by about 0.1 eV . Clearly $(\text{C}_s\text{H}_{\text{BC}}^+)_1$ has the lowest energy in agreement with a number of previous studies which favor $(\text{C}_s\text{H}_{\text{BC}}^+)_1$ (see Refs. 11–13).

The vibrational modes of the carbon-hydrogen complexes are given in Table II, and the bond lengths and angles are given in Table III. $(\text{C}_s\text{H}_{\text{BC}}^+)_1$ gives rise to a hydrogen-

TABLE III. Bond angles (degrees) and bond lengths (\AA) of $(\text{C}_s\text{H}_{\text{BC}}^+)_n$ for $n=1,2,3a,3b$ obtained from the cluster calculation.

	Si-H-Si angle	Si-H bond length	Si-H bond length
H_{BC}^+	178	1.635	1.647
$(\text{C}_s\text{H}_{\text{BC}}^+)_2$	173	1.642	1.645
$(\text{C}_s\text{H}_{\text{BC}}^+)_3a$	137	1.648	1.654
$(\text{C}_s\text{H}_{\text{BC}}^+)_3b$	146	1.634	1.650
	C-H-Si angle	C-H bond length	Si-H bond length
$(\text{C}_s\text{H}_{\text{BC}}^+)_1$	179	1.127	2.255

related mode at 2624 cm^{-1} , which reflects stretching of the C-H bond. For $(\text{C}_s\text{H}_{\text{BC}}^+)_n$ ($n=2,3a,3b$), the H_{BC}^+ stretch mode is lower than that of isolated H_{BC}^+ . The C_{1h} $(\text{C}_s\text{H}_{\text{BC}}^+)_2$ defect has a Si-H-Si angle close to 173° . For $(\text{C}_s\text{H}_{\text{BC}}^+)_3a$ and $(\text{C}_s\text{H}_{\text{BC}}^+)_3b$, the hydrogen atom moves out of the bond center and the Si-H-Si angle becomes 137 and 146° , respectively.

The donor level of $(\text{C}_s\text{H}_{\text{BC}}^+)_1$ was determined using the method described previously.¹⁸ The ionization energy of the defect is compared with that of the C_i defect which is known to possess a donor level at $E_v + 0.28 \text{ eV}$. The $(0/+)$ level for the $(\text{C}_s\text{H}_{\text{BC}}^+)_1$ defect is found to lie at $E_v + 0.22 \text{ eV}$. In $(\text{C}_s\text{H}_{\text{BC}}^+)_n$ ($n=2,3a,3b$) the donor levels are found to lie around $E_c - 0.2 \text{ eV}$.

V. DISCUSSION

Our observations show that the 596 -, 661 -, and 1885-cm^{-1} absorption lines represent local vibrational modes of a defect, denoted CH_I , which involves one hydrogen atom and at least one carbon atom. Carbon is immobile at these low temperatures¹⁹ meaning that a di-carbon defect is very unlikely and, therefore, the defect most probably involves only one carbon atom. The frequencies of the carbon modes at 596 and 661 cm^{-1} are close to the local mode of C_s at 607 cm^{-1} (Ref. 1), and very far from the modes of C_i at 922 and 932 cm^{-1} (Ref. 20). Therefore, we assign the 596 - and 661-cm^{-1} modes to a C_s unit perturbed by a hydrogen atom. Isolated C_s has tetrahedral symmetry and possess one threefold degenerate local mode (T_2). When the symmetry is lowered, the degeneracy is lifted and the C_s unit will have two or three modes. Hence, the observation of two carbon modes indicate by itself that the symmetry of CH_I is lower than tetrahedral, which is consistent with a C_s unit perturbed by a hydrogen atom.

The hydrogen mode at 1885 cm^{-1} lies in the frequency range typical of Si-H stretch modes, well below the range from 2700 to 3100 cm^{-1} associated with the stretching of C-H bonds in molecules.²¹ Moreover, for a C-H stretch mode a significant frequency shift should be observed when ^{12}C is substituted by ^{13}C . As discussed above, this shift is only 0.2 cm^{-1} for the 1885-cm^{-1} mode. For these reasons, we identify the 1885-cm^{-1} mode as a Si-H stretch mode. Actually, the very small dynamical coupling between the carbon and hydrogen atom strongly suggest that the two atoms are rather far apart. The CH_I complexes are primarily formed when isolated H_{BC} becomes mobile as can be seen from Fig. 7, where the intensities of the 1998-cm^{-1} mode (H_{BC}^+) and the 1885-cm^{-1} mode (CH_I) are shown against annealing temperature. The CH_I complex only persists to a slightly higher annealing temperature than isolated H_{BC}^+ , which shows that the thermal stability of CH_I resembles that of H_{BC}^+ . A likely candidate for CH_I is therefore H_{BC}^+ perturbed by a nearby C_s atom. Such a defect should form when H_{BC}^+ starts to migrate and may be expected to be only slightly more stable thermally than isolated H_{BC}^+ . Hence, the stability of CH_I is much lower than that of hydrogen trapped at a vacancy- or interstitial-type defect, which is stable up to at least $\sim 150^\circ\text{C}$.

As mentioned in Sec. III there is evidence for the presence of a second carbon-hydrogen defect, CH_{II} , in our

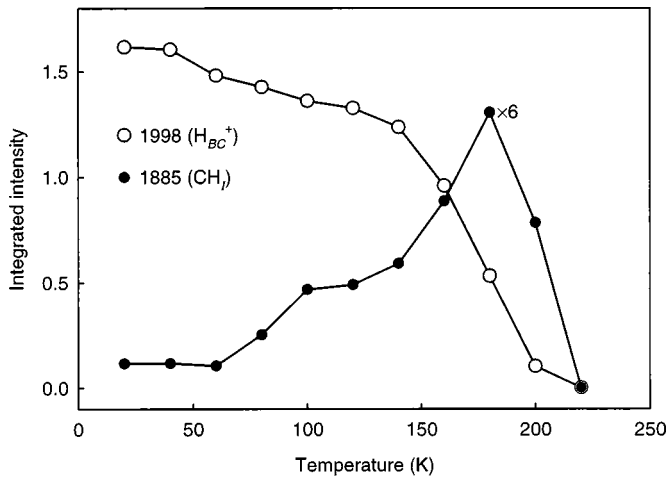


FIG. 7. Intensities of the 1998-cm⁻¹ (H_{BC}⁺) and 1885-cm⁻¹ (CH_I) modes, shown against annealing temperature. The intensity of the 1885-cm⁻¹ mode has been scaled by a factor of 6.

samples. The Si-D stretch mode of CH_{II} at 1363.4 cm⁻¹ is very close in frequency to that of CH_I. It is plausible that CH_{II} has a structure very similar to that of CH_I. Since the frequency of the 1363.4-cm⁻¹ mode does not shift when ¹²C is substituted by ¹³C, the C_s atom is probably more distant from the H_{BC}⁺ atom in CH_{II} than it is for CH_I.

Consider now a carbon-hydrogen defect with a H_{BC}⁺ in the vicinity of a C_s. When a hydrogen atom is placed at a bond-center site in the silicon lattice, the formation of the three-centered Si-H-Si bond leads to reduction of the total energy. However, this is counteracted by the energy needed to increase the Si-Si separation distance in order to accommodate the hydrogen atom at the bond-center site. At some bond-center sites in the vicinity of C_s, less energy is needed to attain the optimum Si-Si distance as compared to an isolated bond-center site. The reason is that the contractive strain field around C_s implies that some of the Si-Si bonds surrounding the C_s will be elongated and thus, less displacement of the two silicon atoms is needed. The net effect is that it is energetically favorable to add a hydrogen atom at such a C_s-perturbed bond-center site. Moreover, the resulting Si-H-Si bond length is longer than for isolated H_{BC}. Consequently, the stretch frequency of H_{BC} at a perturbed site is expected to be lower than for isolated H_{BC}. Our identification of CH_I with a C_sH_{BC}⁺ pair is therefore consistent with the fact that the hydrogen mode falls 113 cm⁻¹ below that of isolated H_{BC}⁺.

Calculation of the effective charge of the hydrogen mode of CH_I supports the assignment of the mode to a H_{BC}⁺ unit. The effective charge η of the mode may be defined by the equation:^{22,23}

$$\int \alpha(\sigma) d\sigma = \frac{\pi \eta^2 N}{n_R c^2 m}, \quad (1)$$

where α is the absorption coefficient, σ the wave number, N the concentration of defects, n_R the refractive index of the material, c the velocity of light, and m the mass of the impurity atom. The Si-C bonds of CH_I resemble those of C_s. Therefore, we expect that the effective charge of the carbon modes of CH_I η_C may be estimated from the corresponding

value for the T_2 mode of C_s. The T_2 mode is three dimensional, so if we assume that the 596- and 661-cm⁻¹ modes together account for three-dimensional vibration, we obtain $\eta_C = \eta_{C_s} = 2.4e$.²⁴ From the maximum intensities of the carbon modes in Fig. 3, we obtain $N = 7 \times 10^{15}$ cm⁻³. Inserting this value of N together with the corresponding intensity of the 1885-cm⁻¹ mode into Eq. (1) allows us to estimate the effective charge of the hydrogen mode, η_H . We obtain $\eta_H = 1.9e$.²⁵ This is a high value for a hydrogen mode in silicon and it is close only to the effective charge of H_{BC}⁺ ($\eta_{H_{BC}} = 1.8e$) (Ref. 15) and of complexes containing hydrogen and group-III acceptors (e.g., $\eta_{Al-H} = 1.9e$) (Ref. 26) and group-V donors (e.g., $\eta_{As-H} = 1.2e$).²⁷ The effective charge of hydrogen in other defects, which do not involve donors or acceptors, is of the order 0.1–0.4e.

From these findings we identify the CH_I defect with H_{BC}⁺ in the vicinity of a C_s atom. The small shift of the 1885-cm⁻¹ mode when the carbon isotope is changed and of the 596- and 661-cm⁻¹ modes when the hydrogen isotope is changed suggest that the carbon and the hydrogen atoms are fairly well separated.

From the *ab initio* calculations we can identify a few possible candidate structures of CH_I. The calculations clearly show that hydrogen is not bound directly to carbon (see Table II), even though (C_sH_{BC}⁺)₁ has the lowest energy, -0.2 eV below the others. It may appear strange why the thermally most stable defect is unobserved. However, we note that ion implantation, in particular at low temperatures, will not leave the sample in thermodynamic equilibrium. It is likely that heat treatment at 220 K, where CH_I anneals out is not sufficient to ensure population of different sites in accordance with their relative energies. The source of hydrogen is probably isolated H_{BC}⁺. Hence, the hydrogen atom has to pass a region with a large number of trap sites surrounding a C_s before it can form (C_sH_{BC}⁺)₁. Therefore, the reaction kinetics may not favor formation of (C_sH_{BC}⁺)₁ in our samples. When CH_I anneals, we would expect (C_sH_{BC}⁺)₁ to form. However, other significantly stronger traps such as vacancy-type defects are also present in significant concentrations. These traps will reduce the formation of closely bound C_s-H complexes. In addition, the calculated effective charge of the hydrogen mode for (C_sH_{BC}⁺)₁ is only 0.33e, whereas those for H_{BC}⁺ and (C_sH_{BC}⁺)₂ are both 1.1e, in fair agreement with the observed values at 1.8 (Ref. 15) and 1.9e. Thus, the hydrogen mode of (C_sH_{BC}⁺)₁ is expected to be about ten times less intense than that of (C_sH_{BC}⁺)₂, if equal concentrations of the defects are present. This may explain why (C_sH_{BC}⁺)₁ has not been observed.

The frequency of the hydrogen mode of (C_sH_{BC}⁺)₂ is lower than that of isolated H_{BC}⁺ by 57 cm⁻¹ (see Table II). This value is comparable to the 113 cm⁻¹ that the CH_I mode falls below that of H_{BC}⁺. The shift of the hydrogen mode when ¹³C substitutes for ¹²C is consistent with the observations. The carbon modes are clearly perturbed by the presence of the H_{BC}⁺ and are split by 83 cm⁻¹, in reasonable agreement with the observed separation of 65 cm⁻¹. Only two carbon modes are observed. However, according to the calculations, one of the carbon modes is located at 574 cm⁻¹, very close to the frequency of C_s at approximately 578 cm⁻¹.

If the weak carbon mode is located that close to the strong C_s mode, it will be nearly impossible to resolve, explaining why it is not observed.

The calculated shifts of the carbon modes when hydrogen is substituted by deuterium range from -0.1 to -3.2 cm^{-1} for $(C_sH_{BC}^+)_2$. These shifts differ somewhat from the observed shifts, which range from -0.3 to -0.5 cm^{-1} . When ^{12}C is replaced by ^{13}C the carbon modes shift by -12 to -19 cm^{-1} in fair agreement with the experimental shifts between -17 and -20 cm^{-1} . Thus, $(C_sH_{BC}^+)_2$ is a possible candidate for CH_1 .

For $(C_sH_{BC}^+)_{3a}$ and $(C_sH_{BC}^+)_{3b}$ the frequencies of the hydrogen modes are lower than that of H_{BC}^+ by 150 and 50 cm^{-1} , respectively. These values are comparable to the observed value of 113 cm^{-1} . The shifts of the carbon and hydrogen modes on isotope substitution are also in reasonable agreement with the observed shifts. However, for $(C_sH_{BC}^+)_{3a}$ and $(C_sH_{BC}^+)_{3b}$ the lowering of the Si-H-Si angle leads to a hydrogen bend mode around 800–900 cm^{-1} , which has not been observed. Therefore, the calculations favor $(C_sH_{BC}^+)_2$ as a plausible candidate for CH_1 . However, $(C_sH_{BC}^+)_{3a}$ and $(C_sH_{BC}^+)_{3b}$ cannot be ruled out completely.

Rather similar complexes, OH_I and OH_{II} were recently observed by infrared-absorption spectroscopy in Czochralski-grown silicon implanted by hydrogen at low (~ 20 K) temperatures. The complexes were identified as a H_{BC}^+ with an interstitial oxygen atom as second, third, or fourth nearest neighbor.¹⁵ Combined with the observations in this work, this suggests that H_{BC}^+ quite generally becomes trapped by nearby defects and impurities such as, e.g., C_i and C_s .

Finally, we shall comment briefly on the identity of the $E3$ center observed by DLTS.^{4,5} According to our calculations, $(C_sH_{BC}^+)_n$ ($n=2,3a,3b$) all possess donor levels

around $E_c - 0.2$ eV, consistent with $E3$,⁴ whereas $(C_sH_{BC}^+)_1$ does not. However, the $E3$ defect has a reported trigonal symmetry,²⁹ which is not in agreement with any of the configurations $(C_sH_{BC}^+)_n$ ($n=2,3a,3b$), but in agreement with $(C_sH_{BC}^+)_1$. The annealing behavior of CH_1 differs somewhat from that of $E3$, indicating that the two centers are not identical.^{4,5} Clearly, further experimental and theoretical input is required to identify the structure of the $E3$ defect. The calculations demonstrate that $(C_sH_{BC}^+)_1$ possesses a $(0/+)$ level at $E_v + 0.28$ eV, in fair agreement with the H_1 center.

VI. CONCLUSION

A carbon-hydrogen complex, CH_1 , has been identified by infrared-absorption spectroscopy. The complex is formed by proton implantation at 20 K, followed by heat treatment at 100–200 K, and it anneals at about 220 K. The complex gives rise to three correlated modes: A hydrogen mode at 1885 cm^{-1} and two carbon modes at 596 and 661 cm^{-1} . The carbon and hydrogen atoms are only weakly coupled. From the observations and *ab initio* calculations, we assign CH_1 to a H_{BC}^+ located at the second or third nearest neighbor site to a C_s .

ACKNOWLEDGMENTS

We thank Lennart Lindström, University of Lund, for providing the ^{13}C -doped silicon samples, and Pia Bomholt for preparing the samples for optical measurements. This work has been supported by the Danish National Research Foundation through the Aarhus Center for Advanced Physics (ACAP). E. V. Lavrov also acknowledges a grant from the Russian Foundation for Basic Research (Grant No. 99-02-16652). S. Öberg thanks NFR and TFR for financial support.

*Permanent address: Institute of Radioengineering and Electronics of RAS, Mokhovaya 11, 103907 Moscow, Russia.

¹R. C. Newman and J. B. Willis, *J. Phys. Chem. Solids* **26**, 373 (1965).

²Y. V. Gorelkinskii and N. N. Nevinyi, *Physica B* **170**, 155 (1991).

³B. Bech Nielsen, *Phys. Rev. B* **37**, 6353 (1988).

⁴A. Endrös, *Phys. Rev. Lett.* **63**, 70 (1989).

⁵Y. Kamiura, N. Ishiga, and Y. Yamashita, *Jpn. J. Appl. Phys., Part 1* **36**, 6579 (1997).

⁶Y. Kamiura, M. Tsutsue, Y. Yamashita, F. Hashimoto, and K. Okuno, *J. Appl. Phys.* **78**, 4478 (1995).

⁷A. N. Safonov, E. C. Lightowers, G. Davies, P. Leary, R. Jones, and S. Öberg, *Phys. Rev. Lett.* **77**, 4812 (1996).

⁸A. N. Safonov and E. C. Lightowers, *Mater. Sci. Eng., B* **58**, 259 (1999).

⁹B. Pajot, B. Clerjaud, and Z.-J. Xu, *Phys. Rev. B* **59**, 7500 (1999).

¹⁰L. Hoffmann, E. V. Lavrov, B. Bech Nielsen, and J. L. Lindström, *Physica B* **273–274**, 275 (1999).

¹¹P. Leary, R. Jones, and S. Öberg, *Phys. Rev. B* **57**, 3887 (1998).

¹²Y. Zhou, R. Luchsinger, P. F. Meier, H. U. Suter, D. Maric, and S. K. Estreicher, *Mater. Sci. Forum* **196–201**, 891 (1995).

¹³C. Kaneta and H. Katayama-Yoshida, *Mater. Sci. Forum* **196–201**, 897 (1995).

¹⁴*Annual Book of ASTM Standards* (ASTM, Philadelphia, 1988), Vol 10.05.

¹⁵B. Bech Nielsen, K. Tanderup, M. Budde, K. Bonde Nielsen, J. L. Lindström, R. Jones, S. Öberg, B. Hourahine, and P. Briddon, *Mater. Sci. Forum* **258–263**, 391 (1997).

¹⁶R. Jones and P. R. Briddon, in *Identification of Defects in Semiconductors*, edited by M. Stavola, Semiconductors and Semimetals Vol. 51A (Academic Press, Boston, 1998), Chap. 6.

¹⁷P. R. Briddon, Ph.D. thesis, University of Exeter, United Kingdom, 1990.

¹⁸A. Resende, R. Jones, S. Öberg, and P. R. Briddon, *Phys. Rev. Lett.* **82**, 2111 (1999).

¹⁹G. Davies and R. C. Newman, in *Handbook on Semiconductors*, edited by T. S. Moss (Elsevier Science, Amsterdam, 1994), Vol. 3b.

²⁰A. R. Bean and R. Newman, *Solid State Commun.* **8**, 175 (1970).

²¹*CRC Handbook of Chemistry and Physics*, 68th ed., edited by R. C. Weast (Chemical Rubber, Boca Raton, FL, 1988), p. F188.

²²R. C. Newman, in *Imperfections in III/V Materials*, edited by E. R. Weber, Semiconductors and Semimetals Vol. 38 (Academic Press, Boston, 1993), p. 117.

²³This formula is only valid for a three-dimensional mode. For a one-dimensional mode a factor of three should be added in the

denominator. However, it is normal procedure to use the formula for all modes, and in order to be able to compare the effective charges we have used Eq. (1).

²⁴S. P. Chappell, M. Claybourn, R. C. Newman, and K. G. Barraclough, *Semicond. Sci. Technol.* **3**, 1047 (1988).

²⁵We note that if we had assumed that the 596- and 661-cm⁻¹ modes account for vibration only in two dimensions, we obtain $\eta_{\text{H}}=1.6e$.

²⁶M. Stavola, S. J. Pearton, J. Lopata, and W. C. Dautremont-Smith, *Appl. Phys. Lett.* **50**, 1086 (1987).

²⁷K. Bergman, M. Stavola, S. J. Pearton, and J. Lopata, *Phys. Rev. B* **37**, 2770 (1988).

²⁸J. D. Holbeck, B. Bech Nielsen, R. Jones, P. Sitch, and S. Öberg, *Phys. Rev. Lett.* **71**, 875 (1993).

²⁹Y. Kamiura, N. Ishiga, and Y. Yamashita, *Jpn. J. Appl. Phys., Part 2* **36**, L1419 (1997).